

Article

Some Sustainability Aspects of Energy Conversion in Urban Electric Trains

Doru A. Nicola ¹, Marc A. Rosen ^{2,*}, Cornelia A. Bulucea ¹ and Constantin Brandusa ³

¹ Faculty of Electromechanical and Environmental Engineering, University of Craiova, Romania; E-Mails: dnicola@em.ucv.ro (D.A.N.); abulucea@gmail.com (C.A.B.)

² Faculty of Engineering and Applied Science, University of Ontario Institute of Technology, 2000 Simcoe Street North, Oshawa, Ontario, L1H 7K4, Canada

³ Electrical Vehicles Department, ROMDATA AQ, Craiova, Romania; E-Mail: rinstalctin@yahoo.com

* Author to whom correspondence should be addressed; E-Mail: marc.rosen@uoit.ca; Tel.: +1-905-721-8668; Fax: +1-905-721-3370.

Received: 1 April 2010; in revised form: 30 April 2010 / Accepted: 6 May 2010 /

Published: 17 May 2010

Abstract: The paper illustrates some aspects of energy conversion processes during underground electric train operation. Energy conversion processes are explained using exergy, in order to support transport system sustainability. Loss of exergy reflects a loss of potential of energy to do work. Following the notion that life in Nature demonstrates sustainable energy conversion, we approach the sustainability of urban transportation systems according to the model of an ecosystem. The presentation steps based on an industrial ecosystem metabolism include describing the urban electric railway system as an industrial ecosystem with its limits and components, defining system operation regimes, and assessing the equilibrium points of the system for two reference frames. For an electric train, exergy losses can be related to the energy flows during dynamic processes, and exergy conversion in these processes provides a meaningful measure of the industrial (*i.e.*, transportation) ecosystem efficiency. As a validation of the theoretical results, a case study is analyzed for three underground urban electric train types REU-U, REU-M, REU-G operating in the Bucharest Underground Railway System (METROREX). The main experimental results are presented and processed, and relevant diagrams are constructed. It is determined that there is great potential for improving the performance of rail systems and increasing their sustainability. For instance, power converters and efficient anti-skid systems

can ensure optimum traction and minimum electricity use, and the recovered energy in electric braking can be used by other underground trains, increasing exergy efficiency, although caution must be exercised when doing so to avoid reducing the efficiency of the overall system.

Keywords: urban electric transportation; sustainability; electric train; energy conversion; exergy; induction motor; industrial ecology

Notation

f_s (f_N)	stator frequency (rated stator frequency) [Hz]
f_{2wR} , f_{2wS} , f_{2wT}	commutation functions with two levels
i	transmission ratio of gear reducer
i_{d2}	input current of VVVF inverter [A]
i_R , i_S , i_T	output currents of VVVF inverter [A]
m	railway vehicle mass [t]
n	rotor speed [rpm]
p	poles pair number of induction motor
r	specific train resistance [daN/t]
r_{ps} , i_{dc} , r_c	specific main resistance, specific resistance caused by declivities and specific resistance caused by curves [daN/t]
u_d	input voltage of VVVF inverter [V]
u_{Nn}	zero-sequence voltage [V]
\underline{u}_s , \underline{i}_s , \underline{i}_r'	space-phasors of stator voltages, stator currents and rotor currents (reduced to stator)
u_{Rn} , u_{Sn} , u_{Tn}	output voltages of VVVF inverter [V]
z	traction motors number
C2Q	two quadrants converter
D_r	wheel diameter [m]
F	total traction force [N]
F_0	active motor force at rim [kN]
F_F	braking force at rim [kN]
$G_{ad} = m_{ad} \cdot g$	adherent weight of railway vehicle [N]
IT2N	two levels VVVF inverter
$L_F C_F$	input filter (network filter)
L_s , L_r' , L_u	stator, rotor and useful (magnetizing) cyclical inductances [H]
M (M_k , M_N)	electromagnetic torque (maximum electromagnetic torque, rated electromagnetic torque) [Nm]
M_2	useful torque of traction induction motor [Nm]
MAT	traction asynchronous motor
MW	motor wagon

P_0	active power at rim [kW]
R	total resistance to train running [N]
R_s	phase stator winding resistance [Ω]
R_r'	rotor resistance reduced to stator [Ω]
U_1, I_1	supply line voltage and RMS current of induction motor [V], [A]
$U_s (U_N)$	RMS phase stator voltage (RMS rated stator voltage) [V]
VVVF	Variable voltage variable frequency
$\xi = 1 + \sigma$	inertia constant of railway vehicle
φ	adherence coefficient
η_t	transmission efficiency of gear reducer
$\omega_m = 2\pi n/60$	mechanical angular frequency [elect.rad/s]
$\omega_r = \omega_s - \omega_m$	rotor angular frequency [elect.rad/s]
$\omega_s = 2\pi f_s (\omega_N)$	stator angular frequency (rated stator angular frequency) [elect.rad/s]
σ	leakage coefficient of induction machine (Blondel coefficient)
Ω_m	mechanical angular speed of traction motor rotor [rad/s]
$\Psi_s (\Psi_{sN})$	stator total flux (rated stator total flux) [Wb.turn]
$\underline{\Psi}_s, \underline{\Psi}_r'$	space-phasors of stator fluxes and rotor fluxes (reduced to stator)

1. Introduction

To address meaningfully many of the problems facing humanity today, conditions for the performance of sustainable technical systems must be formulated. Real processes involving energy and materials need to be linked to environmental impact as well as engineering design and operation. Correspondingly, exergy concepts can help understand the efficiencies of electromechanically driven systems and guide improvement efforts [1,2]. Here, the applicability of exergy methods to underground electrical railway transport systems is described.

The merit of an urban electric transportation system is based not only on technical performance, safety, energy efficiency, economics and societal acceptance, but also on environmental impact and exergy efficiency. Costs should reflect value, which is associated not with energy but rather with exergy and sustainability. While energy is a measure of quantity only, exergy is a measure of quantity and quality or usefulness [3]. This study of underground electric trains is based on the concept that the efficiency reduction from large exergy destructions and the corresponding long-term environmental degradation can be understood and improved by viewing the electric train as an industrial ecosystem. This research extends earlier work by the authors [4,5].

Much other research has been reported on the application of exergy in seeking sustainable transport. For instance, exergy has recently been used to assess the transport sectors in Greece [6] and the United Kingdom [7]. Some studies have focused on applying exergy to rail transport. For example, exergy has been used to investigate the Italian railway transport system [8] and electric transport devices using fuels like liquefied natural gas [9].

Increasing efforts are being expended to enhance the sustainability of transportation technologies and systems. For instance, approaches to and issues in sustainable transport systems have been

explored [10,11], as have policy requirements to achieve sustainable urban transport [12]. Research to improve rail transport sustainability has also received increased focus, with initiatives reported on innovative lightweight transit technologies [13] and combining electric vehicles with intermodal transport [14]. Some of these efforts have focused on reducing the environmental impact of rail transport by reducing emissions of greenhouse gases and other pollutants [15].

Following the above context, this paper describes the electric design of urban rail transportation systems as well as their characteristics and performances, considering their drive systems with induction motors supplied at variable frequency with controlled stator flux. After modeling the main traction equipment, *i.e.*, induction motors and variable voltage variable frequency (VVVF) inverter, the design of a structural diagram of the main electric circuits on urban electric trains is presented, together with the structural model of useful movement. Finally, on the basis of a particular case, the energy consumption is validated in this paper corresponding to a complete cycle (*i.e.*, acceleration, constant running speed and deceleration) for the analyzed underground train.

2. Energy Conversion in Urban Electric Trains

At the start, we adopt a dualist view [16], in which the transportation system is taken to be surrounded by two environments: technical and ecological. The electric transportation system is closed within the technical surroundings, but open within the ecological environment.

Modern urban electric railway trains are supplied by a d.c. contact line and are equipped with three-phase induction motors and variable voltage variable frequency (VVVF) inverters [17]. Since electric drive systems are used with static converters and traction induction motors, with appropriate controls these machines can realize both traction and electric braking regimes of electric traction vehicles. Utilization in electric traction of an induction motor with a rotor squirrel cage is possible only in the conditions of a three-phase supply system with controlled variable frequency and r.m.s. voltages [18].

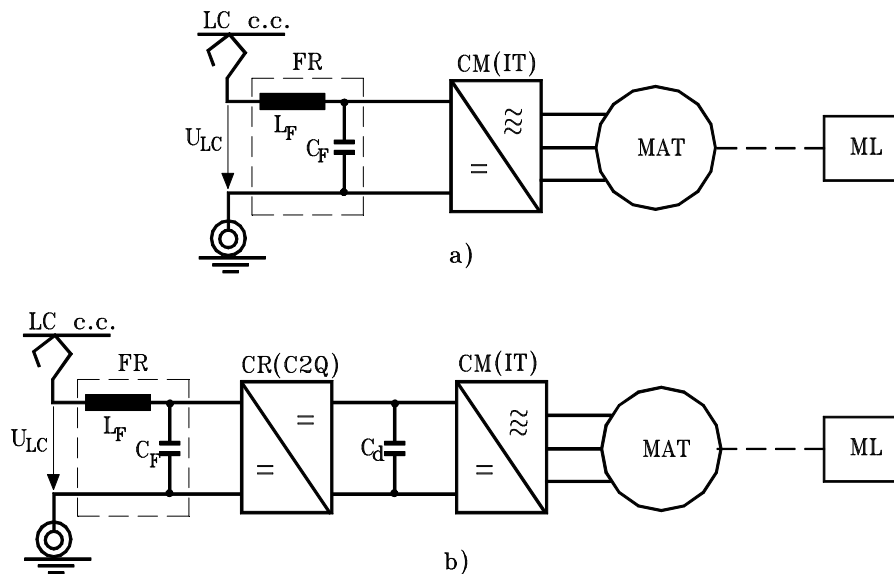
This supply type is achieved with a machine-side converter (CM), usually a VVVF inverter (IT) with two or three levels (Figure 1). The working mechanism (ML) represents the mechanical part of the motor electric vehicle that it is located between a movement transformer (reduction gear) and a movement converter (wheel + rail) which transforms rotation into translational movement.

But, to commence, we need to know in what way electric traction drive systems based on static converters lead to an improvement in electric train performance, regarding both optimum traction characteristics (in terms of energy use) and high exergy efficiency in train operation, particularly for electric braking with energy recovery.

2.1. Operation at Variable Frequency of Induction Machine

An industrial ecosystem does not have a single equilibrium point [19]. Rather, the system moves among multiple stable states [20]. The dynamic regimes in electric train operation, *e.g.*, starting or braking processes, can be viewed as representing the industrial ecosystem movement among points of equilibrium.

Figure 1. Principal scheme of main electric circuits of urban electric trains fed by a d.c. contact line.



Vehicle regulation speed is determined examining the static converter (VVVF) and electric machine as an assembly [21]. The traction motor speed regulation is based on stator voltage and frequency variation, so that to achieve high energy efficiency, the first requirement of the train control system concerns passing of the motor operation equilibrium point from one mechanical characteristic to another.

In the range of frequencies lower than the rated frequency, $f_s < f_N$, in order to ensure a constant level of inductor machine stator flux $\Psi_s = \Psi_{sN}$, we have to simultaneously modify the frequency f_s and the supply voltage magnitude U_s so the supply r.m.s. voltage U_s varies with the frequency f_s according to $U_s(f_s) = |R_s I_s + j2\pi f_s \Psi_{sN}|$, where R_s is the stator resistance and Ψ_s the stator flux.

In the case considered subsequently of an induction machine supplied by a variable frequency voltage source, when the rated speed is reached (*i.e.*, the induction motor is supplied at U_N and f_N) a further increase in speed is possible only by increasing the stator frequency magnitude over the rated frequency $f_s > f_N$. Note that because of the voltage restriction on both converters and induction machine winding insulation considerations, the stator voltage is limited and maintained at a constant magnitude $U_s = U_N$ for the entire high frequency domain, and the induction machine operates in weakened flux conditions [17]. From an energetic viewpoint it is noted that, because the stator flux and pulsation exhibit an inverse proportionality relation $\Psi_s = U_N/\omega_s$, the machine torque capability is strongly affected, and the energy destruction can not be avoided.

We conclude that the induction machine supplied from a variable frequency and voltage source operates with full field $\psi_s = \psi_{sN} = \text{const.}$ in the low frequency range $f_s \leq f_N$ and with a weakened field ($\psi_s < \psi_{sN}$) in the increased frequency domain $f_s > f_N$ (when the supply r.m.s. voltage remains constant ($U_s = U_N = \text{const.}$)).

2.2. Electric Train with Induction Motors Operating at Variable Frequency and Controlled Flux

The operation at variable frequency with controlled flux is preceded for induction motors in drive systems with vectorial control [22]. The vectorial regulation and control method is based on space phasor

theory, taking into consideration the control of both the flux and the induction machine electromagnetic torque M . In principle, the stator current space phasor is decomposed into two perpendicular components (a flux component and a torque component) which are separately controlled. In this paper we analyze the steady-state sinusoidal regime of variable frequency operation with *controlled stator flux*. Note that the theoretical developments presume an induction machine with constant parameters, without iron losses and without saturation of the magnetic core.

In the steady-state the following relations can be derived for the stator current components [23]:

$$\begin{aligned} I_{sx} &= \frac{\psi_s}{L_s} + \frac{1-\sigma}{\sigma L_s} \frac{\psi_s}{\frac{R_{r'}}{\omega_r \sigma L_{r'}} + \frac{\omega_r \sigma L_{r'}}{R_{r'}}} \\ I_{sy} &= \frac{1-\sigma}{\sigma L_s} \frac{\psi_s}{\frac{R_{r'}}{\omega_r \sigma L_{r'}} + \frac{\omega_r \sigma L_{r'}}{R_{r'}}} \end{aligned} \quad (1)$$

The absolute value of the stator current can be determined with the formula $I_s = (I_{sx}^2 + I_{sy}^2)^{1/2}$.

Within the ecological framework, the electromagnetic torque M is again related to the system output exergy. We can express M in complex coordinates axes system (oriented on $\underline{\psi}_s$) as

$$\begin{aligned} M &= 3p \cdot \text{Im}\{I_s \cdot \underline{\psi}_s^*\} = \\ &= 3p \cdot \text{Im}\{(I_{sx} + jI_{sy}) \cdot \underline{\psi}_s\} = \\ &= 3p \cdot \psi_s \cdot I_{sy} \end{aligned} \quad (2)$$

Substituting I_{sy} from (1), the torque relation becomes

$$M = 3p \cdot \frac{1-\sigma}{\sigma L_s} \cdot \frac{\psi_s^2}{\frac{R_{r'}}{\omega_r \sigma L_{r'}} + \frac{\omega_r \sigma L_{r'}}{R_{r'}}} \quad (3)$$

If the stator flux ψ_s is constant, the electromagnetic torque magnitude depends on the rotor current pulsation ω_r but not the stator supply frequency f_s . The torque curve $M = f(\omega_r)$ at $\psi_s = \text{const.}$ is not linearly dependent on ω_r , having two symmetrical extremes:

$$\begin{aligned} \frac{\partial M}{\partial \omega_r} &= 0; \quad \omega_{rk\psi_s} = \pm \frac{R_{r'}}{\sigma \cdot L_{r'}}; \\ M_{k\psi_s} &= M(\omega_{rk\psi_s}) = \pm \frac{3p}{2} \cdot \frac{1-\sigma}{\sigma \cdot L_s} \cdot \psi_s^2 \end{aligned} \quad (4)$$

The dependence of $M = f(\omega_r)$ at $\psi_s = \text{const.}$ is shown in Figure 2.

In a steady-state regime, a system stable operation (with $\partial M / \partial \omega_r > 0$) is performed only on the ascendant zone of the characteristic $M = f(\omega_r)$ in Figure 2 and corresponds at small rotor pulsations to the condition $|\omega_r| \leq \omega_{rk\psi_s}$. The mechanical characteristics family $M = f(n)$ of the induction motor operating at $\psi_s = \text{const.}$, for different stator frequencies f_s are shown in Figure 3.

Figure 2. Torque characteristic $M = f(\omega_r)$ at controlled stator flux.

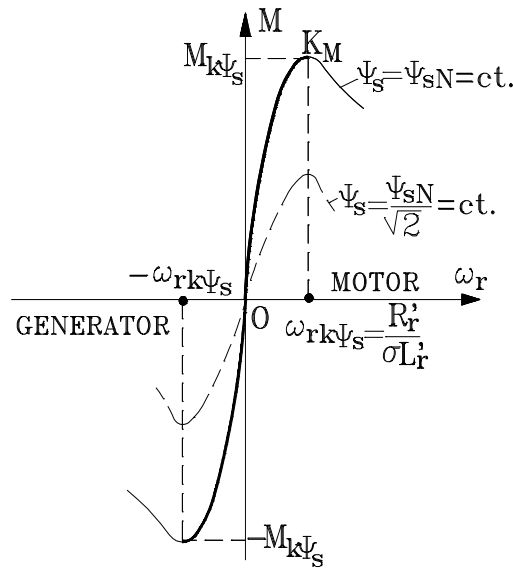
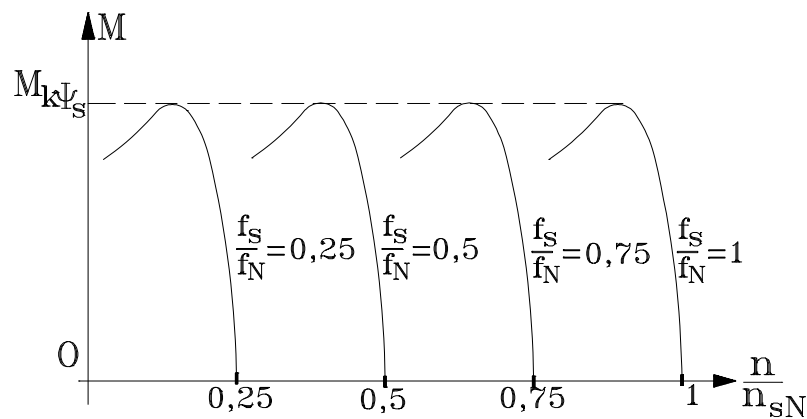


Figure 3. Mechanical characteristics $M = f(n)$ at $\psi_s = \text{const.}$ for different frequency values $f_s \leq f_N$.



The constant stator flux magnitude ψ_s for any stator frequency f_s and torque M (respectively, any rotor pulsation ω_r) imposes an exact control of either the supply voltage U_s or the supply current I_s . We see again an analogy between this electrical system and an ecosystem. *An appropriate technical system control must be achieved for reducing exergy destruction when the equilibrium point passes from one stable state (represented by the operation point on a certain mechanical characteristic) to another stable state (on another mechanical characteristic).* This observation implies the system control needs to be assessed next.

2.3. Modeling of Electric Train

Observations of nature suggest we need to identify modalities for optimum train control to minimize energy consumption and maximize exergy efficiency. We know the shape of the ideal traction characteristic [17]. The real traction characteristic identifies if the train control is appropriate. To achieve vehicle control requires an analysis based on *structural diagrams*.

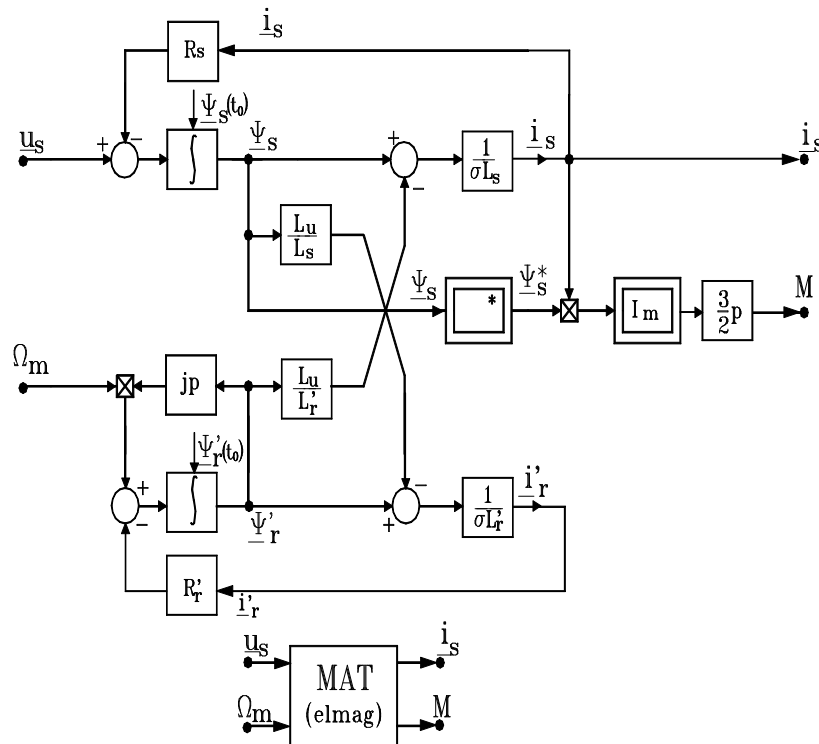
First, we model the traction induction motor, where electromechanical energy conversion occurs. As a complex electromechanical system, the induction motor can be conceptually decomposed into electromagnetic and mechanical subsystems. Between these functional parts, the electromagnetic torque M and the rotor mechanical speed Ω_m interact as internal variables. The induction motor electromagnetic part can be described by the following equations [17]:

$$\begin{aligned} \frac{d\Psi_s}{dt} &= \underline{u}_s - R_s \cdot \underline{i}_s \\ \frac{d\Psi_r'}{dt} &= j \cdot p \cdot \Omega_m \cdot \underline{\Psi}_r' - R_r' \cdot \underline{i}_r' \\ \underline{i}_s &= \frac{\underline{\Psi}_s - \frac{L_u}{L_r'} \cdot \underline{\Psi}_r'}{\sigma L_s}; \quad \underline{i}_r' = \frac{\underline{\Psi}_r' - \frac{L_u}{L_s} \cdot \underline{\Psi}_s}{\sigma L_r'} \\ M &= \frac{3}{2} \cdot p \cdot \text{Im}\{\underline{i}_s \cdot \underline{\Psi}_s^*\} \end{aligned} \tag{5}$$

Here, \underline{u}_s denotes the stator voltage vector; \underline{i}_s the stator current vector; \underline{i}_r' the rotor current vector; $\underline{\Psi}_s$ the stator flux vector; $\underline{\Psi}_r'$ the rotor flux vector; L_u the magnetizing inductance; L_s the stator inductance; L_r' the rotor inductance; p the number of pole pairs; R_s the stator resistance; R_r' the rotor resistance and $\sigma = 1 - \frac{L_u^2}{L_s \cdot L_r'}$ the motor leakage coefficient.

Using Equation (5), the structural diagram and the mask block of the induction motor electromagnetic part can be represented (Figure 4).

Figure 4. Structural diagram and mask block for induction motor electromagnetic part.



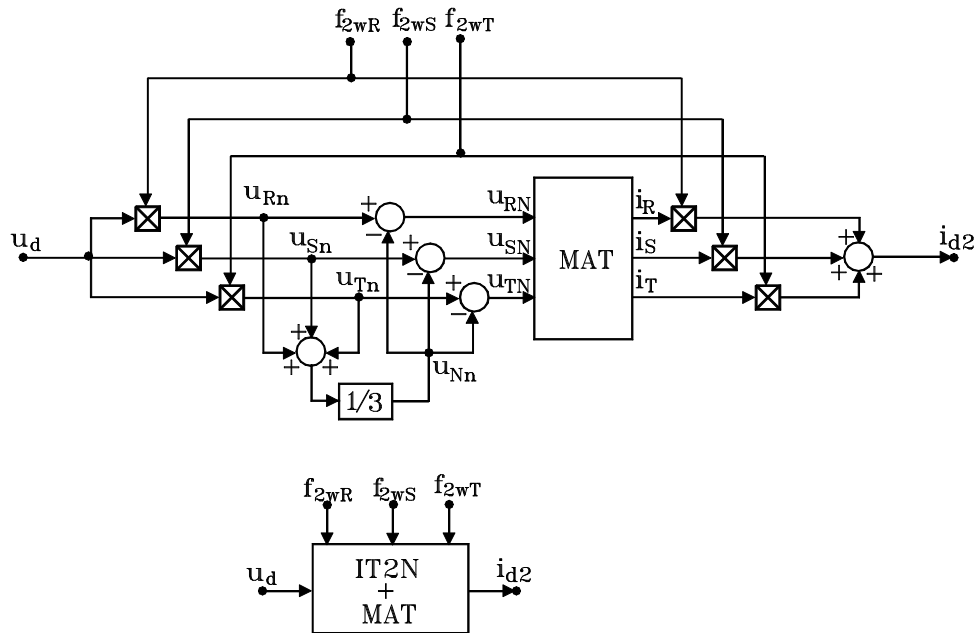
The structural diagram of the electromagnetic subsystem can be coupled both with the structural diagram of the VVVF inverter through the input variable \underline{u}_s and output variable \underline{i}_s and with the structural diagram of the mechanical subsystem via the input quantity Ω_m and the output quantity M .

To model the machine-side converter, usually a voltage-source inverter, commutation functions are used in two or three levels, respectively [17,18]. A static converter can be viewed for modeling as a “black box” with input/output characteristics through the commutation functions. Analysing the topology of a three-phase voltage-source inverter with two levels and using the commutation function f_{2w} (in two levels), $f_{2w} = \begin{cases} 1 \\ 0 \end{cases}$, for each arm of converter, equations for the inverter model (without losses) can be written as:

$$\begin{aligned} u_{Rn} &= u_d \cdot f_{2wR}; \quad u_{Sn} = u_d \cdot f_{2wS}; \quad u_{Tn} = u_d \cdot f_{2wT}; \\ i_{d2} &= i_R \cdot f_{2wR} + i_S \cdot f_{2wS} + i_T \cdot f_{2wT}; \\ u_{RN} &= u_{Rn} - u_{Nn}; \quad u_{SN} = u_{Sn} - u_{Nn}; \quad u_{TN} = u_{Tn} - u_{Nn}; \\ u_{Nn} &= \frac{u_{Rn} + u_{Sn} + u_{Tn}}{3}; \end{aligned} \tag{6}$$

With this system of equations, the structural diagram and mask block of the three-phase voltage-source inverter with two levels are obtained (Figure 5).

Figure 5. Structural diagram and mask block for three-phase voltage source inverter with two levels.



To highlight the exergetic dynamic approach of the system, a *vehicle useful movement model* is also necessary [17]. Here, we consider a motor electric vehicle with mass $m[t]$ and inertia constant ξ having a specific train resistance $r[daN/t]$. If movement occurs due to the action of useful torques M_2 (identical), developed by z vehicle traction motors of the motor electric, then the useful movement can be described as:

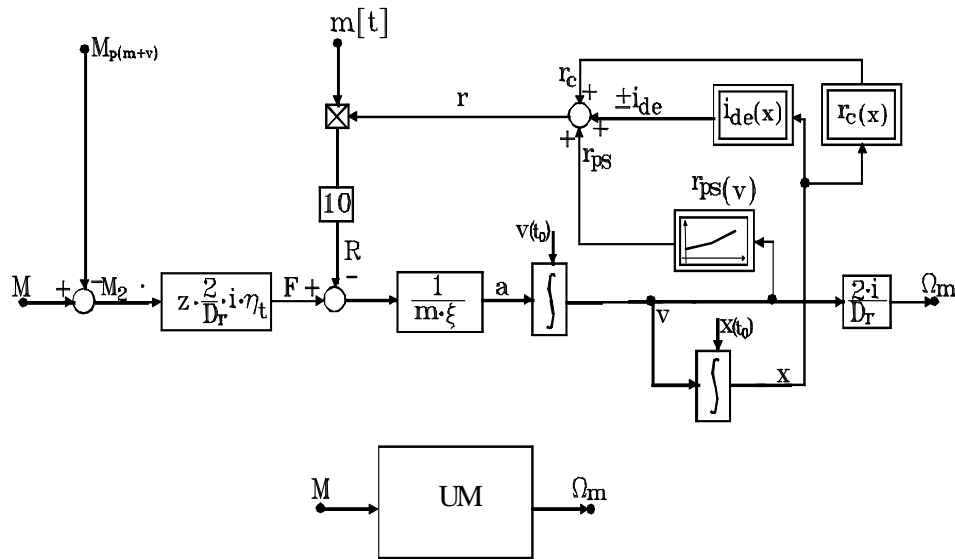
$$v = \frac{1}{m \cdot \xi} \int (F - R) dt ; \Omega_m = \frac{2 \cdot i}{D_r} \cdot v ; x = \int v \cdot dt$$

$$F = z \cdot \frac{2}{D_r} \cdot i \cdot \eta_t \cdot M_2$$

$$R = (r_{ps}(v) \pm i_{de}(x) + r_c(x)) \cdot m \cdot 10$$
(7)

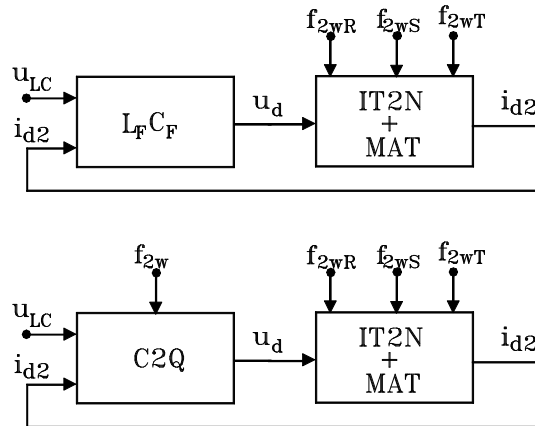
which allow the construction of the structural diagram of useful movement (Figure 6). For the mask block, we considered as an input quantity the torque M and as an output quantity the speed Ω_m , *i.e.*, the time-varying quantities during useful movement.

Figure 6. Structural diagram and mask block of useful movement.



Subsequently, diagrams of train running speed $v(t)$ and distance $x(t)$ can be developed. Modifications to vehicle mass and dependences $i_{de}(x)$ or $r_c(x)$, specific to a vehicle or route, can be incorporated, yielding an exact model for all operating conditions.

Figure 7. Structural diagrams of main electric circuits.



We began our study considering the main circuits of electric trains fed from a d.c. contact line (Figure 1) and have obtained its structural diagrams (Figure 7). This information supports the aim of optimizing vehicle control to obtain a high exergy efficiency.

3. Case Study

In this case study we consider an urban electric train with two motor wagons (MWs) which are elastic coupled and which are referred to as “MW + MW” [23]. The vehicle electric scheme (Figure 8) is in variant V2, which is defined by the coefficient $K = 2/2$, indicating two static converters, each supplying two traction bi-motors. On the basis of the previous structural diagrams, the structural diagram for the urban electric vehicle viewed as a system is assessed in Figure 9.

The electric traction scheme with a power supply from a d.c. network has the following elements [17,23]: a current connector to a third rail; a loading contactor and a loading resistor; a rapid automatic circuit breaker; an input circuit (known as a LC filter); a voltage and frequency converter; electric traction motors; a braking chopper and a braking resistor and a shunt; and electric couplings for the wagons.

From the technical point of view, the electric traction scheme presented here meets the criteria of vehicle operating safety and traction scheme reliability. An understanding of the sustainability of the electric transportation system can be obtained with an analysis of the exergy conversion chain within the electric transportation system operation regimes.

Figure 8. Electric traction diagram in variant $K = 2/2$.

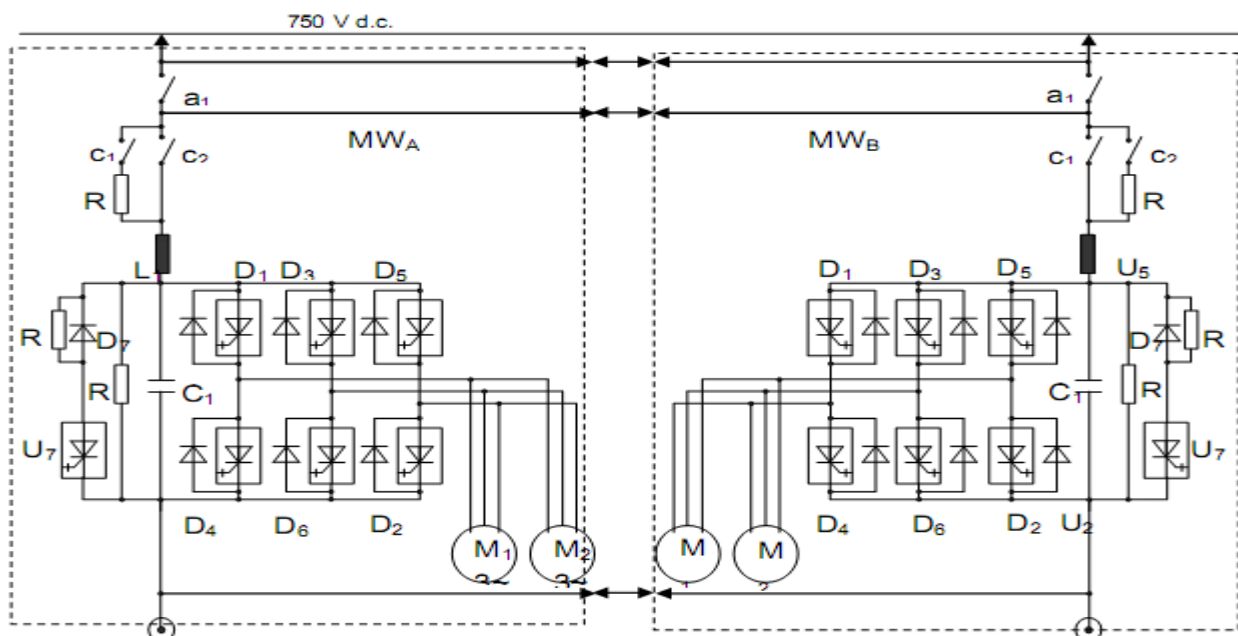
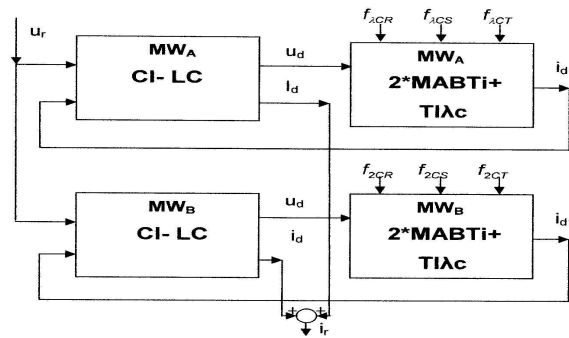


Figure 9. Structural diagram of urban electric vehicle MW + MW, with $K = 2/2$.



Here, the train operation is briefly described. After the connectors coupling, the circuit breakers and contactors switching, the control of the unit's inverters is determined. The traction induction bi-motor groups are supplied from the three-phase VVVF inverters. Consequently, the urban electric train is able to operate. At the minimum adjusted frequency $f_{min} = sf_n$, the traction motors M_1 and M_2 on the first unit MW_A are immobile. Similarly M_1 and M_2 are placed on the second unit MW_B .

When the frequency exceeds that value, the motors start to move, with the operation following the frequency mechanical characteristic corresponding to the minimum supply frequency. The electric train accelerates at a constant traction torque, with operation on the mechanical characteristics at up to f_{sn} , when $U_1 = U_{1n}$ and then, over f_{sn} , at constant power.

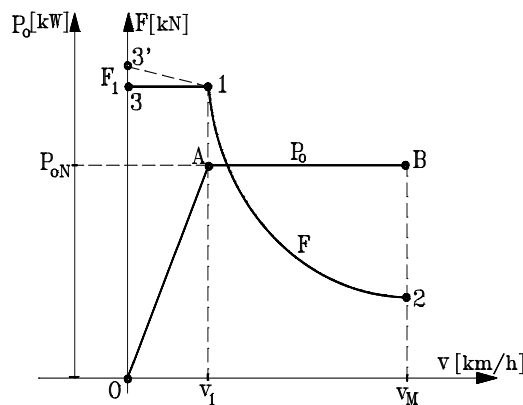
The three-phase traction induction motors reverse their rotation via a simple supply commutation, by stator phases succession switching. The motors have identical characteristics for both rotation senses.

It is emphasized that *exergy issues prefer the vehicle electric motors operate at the designed rating power for a running speed range as long as possible* [17]. Hence, the active power at rim P_0 is constant and the active force F depends on the speed according to

$$F[\text{kN}] = 3.6 \cdot \frac{P_0[\text{kW}]}{v[\text{km/h}]} \tag{8}$$

On basis of equation (8), a hyperbole form of the active force F results, as shown in Figure10.

Figure 10. Ideal mechanical characteristic.



From the viewpoint of exergy efficiency and environment issues, a special aspect in case of the non-autonomous vehicles with electric traction is represented by the braking regime, particularly *electric braking*. Since electric driving systems with static converters and traction induction motors are used, electric braking with the same motors can be realized with appropriate control for electric traction vehicles. For a specified running direction, passing from the traction regime to the electric brake regime corresponds to a sign change of the active force F . Clearly in the traction regime the vehicle speed v and the active force F have the same sign, while in the braking regime v and F have opposite signs.

To perform electric train braking, the traction induction motors pass into the electric generator regime, by decreasing control of the supply voltage frequency. The electric traction machines operate in the generator regime on the mechanical characteristics $M = f(n)$ in quadrants II and IV (Figures 2 and 3), respectively. In that situation, which is complex from the viewpoint of power circulation, the inverter provides the reactive energy for the traction machine in the generator regime using the capacitor battery from the LC circuit and through the recovery diodes group, and the electrical machine supplies power like an induction generator into the d.c. network. This recovered energy is used by other operating trains. Thus the exergy efficiency is high. The d.c. network capacity to receive this electric energy is continuously checked by the vehicle control system. If the input circuit voltage exceeds $1.2U_d$ (i.e., over $1.2 \times 750 = 900$ V), braking choppers are automatically activated, which realize an electric rheostatic brake regime. The braking resistances allow energy dissipation (by the Joule effect) of the uncirculated electric energy. Then, a high energy efficiency of the brake resistances is obtained, but the system exergy efficiency is significantly decreased.

The environmental impacts from the electric braking regime, particularly with recovered energy, by shifting the traction machines to an electric generator regime, are considerably reduced.

4. Experimental Results

The Bucharest Underground Railway System (METROREX) has trains equipped with traction induction motors MAB T_1 , MAB T_2 and MAB T_3 produced by the Electroputere Factory in Craiova. The following railway vehicles types are considered:

- urban electric train—heavy implementation REU-G with a weight of 36 t/wagon,
- urban electric train—medium implementation REU-M, with a weight of 25 t/wagon, and
- urban electric train—light implementation REU-U, with a weight of 15 t/wagon.

For REU-G, experimental traction characteristics are plotted in Figure 11, showing the variations of characteristics are similar, suggesting *the goal of minimum energy consumption in the traction regime is accomplished*. Data are provided in Table 1.

Figure 11. Variation of Rp, Po, Fo and v for REU-G.

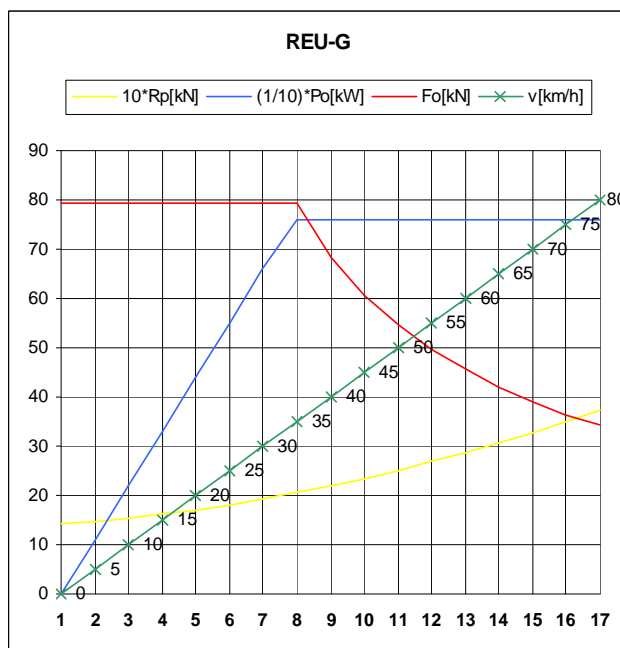


Table 1. Values of Rp, Po, Fo and v for REU-G.

Rp [N]	Po [kW]	Fo [kN]	v [km/h]	Reading number
1,419	0	79.27	0	1
1,474	110	79.27	5	2
1,539	220	79.27	10	3
1,617	330	79.27	15	4
1,709	440	79.27	20	5
1,812	550	79.27	25	6
1,926	661	79.27	30	7
2,053	760	79.27	35	8
2,194	760	68.37	40	9
2,344	760	60.77	45	10
2,508	760	54.70	50	11
2,684	760	49.72	55	12
2,872	760	45.60	60	13
3,070	760	42.07	65	14
3,281	760	39.07	70	15
3,506	760	36.46	75	16
3,743	760	34.18	80	17

Experimental electric braking characteristics for three train types REU-U, REU-M, REU-G used by the Bucharest Underground Railway System are presented in Figure 12 and Table 2.

Figure 12. Variations of forces F_F and speed v in electric braking regime for vehicles REU-U, REU-M, REU-G.

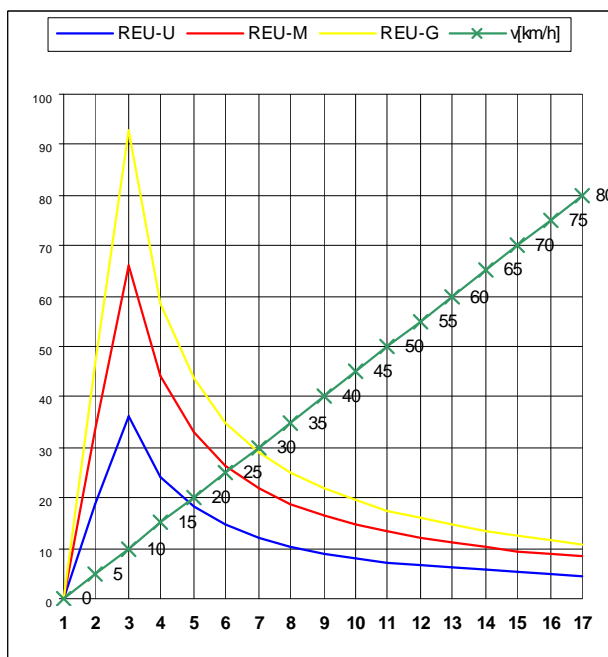


Table 2. Experimental electric braking characteristics for three train types.

REU-U F_F [kN]	REU-M F_F [kN]	REU-G F_F [kN]	v [km/h]	Reading number
0.00	0.00	0.00	0	1
18.78	33.56	46.36	5	2
36.36	66.24	92.71	10	3
24.24	44.16	58.32	15	4
18.18	33.12	43.74	20	5
14.55	26.50	34.99	25	6
12.12	22.08	29.16	30	7
10.39	18.93	24.99	35	8
9.09	16.56	21.87	40	9
8.08	14.72	19.44	45	10
7.27	13.25	17.49	50	11
6.61	12.04	15.90	55	12
6.06	11.04	14.58	60	13
5.59	10.19	13.46	65	14
5.19	9.46	12.50	70	15
4.85	8.83	11.66	75	16
4.55	8.28	10.93	80	17

The Urban Underground Railway Transportation System in Bucharest is a network of four lines (M1, M2, M3 and M4) with 49 train stations and a total length of 67 km. Trains travel between 5 a.m. and 11:30 p.m., with an average frequency of 10 minutes.

In our calculations we assume the following:

- a 1,560 m length between consecutive stations,
- a running time between consecutive stations of 96 s, with 20 s transient starting (10 s at constant force and 10 s at constant power), 60 s of constant speed running and 16 s electric braking, and
- electric active energies as in Table 3, following the electric active power P values in Figure 13.

During deceleration (interval 80–96 s), the electric active power (3,000 kW) corresponds to recovered energy or heat, depending on electric brake type.

An analysis of the recovered energy indicates that on a railway segment at least three trains must be in operation (two at speeds higher than 10 m/s and one in a uniform electric brake regime). So, for high exergy efficiency, the number of trains operating on a rail segment should be $n = [3,000/2,400] \times 2$.

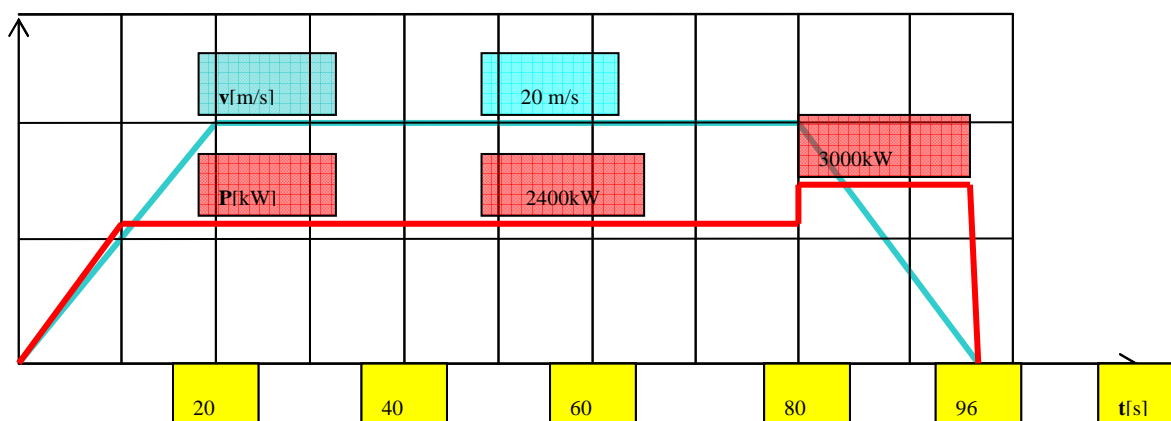
5. Discussion

The train case study considered yields particularly useful results in the traction regime. Using structural diagrams and high-performance converters, appropriate vehicle control can be achieved so the train experimental dynamic characteristics follow the theoretical mechanical characteristic. Then, the energy and exergy efficiencies are equal. Power converters and efficient anti-skid systems ensure optimum traction and minimum energy use.

Table 3. Data for railway system.

Parameter	Value
Railway length	1,560 m
Cycle time	96 s
Train number	1
Electric frames number	3
Number of wagons	$3 \times 2 = 6$
Number of motors	$6 \times 4 = 24$
Installed power, P	2,400 kW
Running speed, v_o	20 m/s
Acceleration time, t_{ac}	20 s
Uniform running time, t_{ur}	60 s
Deceleration time, t_{dc}	16 s
Electric energy in acceleration regime, E_{ac}	36,000 kWs (10 kWh)
Electric energy in uniform running regime, E_{ur}	144,000 kWs (40 kWh)
Electric energy in deceleration regime, E_{dc}	48,000 kWs (13 kWh)

Figure 13. Variation with time of speed and supplied electric active power for a complete cycle: acceleration, constant speed running and deceleration.



Concerning train electric braking, further research is needed on the transportation system internal exergy consumptions. Actual techniques allow driving systems to be implemented on the basis of variable voltage and frequency static converters and induction motors, which facilitate improved electric braking, even with energy recovery. In that operating regime, the vehicle provides energy to the d.c. network through an inverter. The recovered energy is used by other underground trains, increasing exergy efficiency.

Another result related to exergy efficiency improvement relates to the railway transportation system traffic intensity and may seem paradoxical. At present, the energy recovered from electric braking can be provided only to running trains in the transportation system. As the number of running trains in the system increases, the exergy efficiency is high if the recovered electric energy is properly used. But with few running trains, if the third rail voltage exceeds 900 V, the rheostatic brake regime is automatically controlled and the recovered electric energy is transformed by the Joule Effect to heat. This is an unfavorable situation, with adequate energy efficiency, but a low exergy efficiency.

Electric braking with energy recovery should be compulsory in the long run in electric transportation systems to improve their sustainability, and the elasticity of reversible traction sub-station equipment should be taken into account.

The results are expected to help make electrical transportation systems more sustainable.

6. Conclusions

Energy systems involving conversion chain processes often are highly irreversible and have low exergy efficiencies. Within an Industrial Ecology framework there is great potential for improving the performance of such technical systems and increasing their sustainability. For instance, power converters and efficient anti-skid systems can ensure optimum traction with minimum electricity use, while energy can be recovered effectively via electric braking for use in other underground trains, increasing exergy efficiency. Further research is needed on the transportation system internal exergy efficiencies and consumptions related to train electric braking. Care must be exercised when implementing exergy efficiency improvements due to potential negative effects related to railway transportation system traffic intensity, which can lead to an adequate energy efficiency but a low

exergy efficiency. Electric braking with energy recovery should be compulsory in the long run in electric transportation systems to improve their sustainability, and the elasticity of reversible traction sub-station equipment should be taken into account. If applied, the results of this investigation can help make electrical transportation systems more sustainable.

Acknowledgements

Financial support was provided by the Natural Sciences and Engineering Research Council of Canada.

References and Notes

1. Rosen, M.A. A Concise Review of Energy-Based Economic Methods. In *Proceedings of the 3rd IASME/WSEAS International Conference on Energy & Environment*, Cambridge, UK, 23–25 February 2008; pp. 136-142.
2. Allenby, B.R. *Industrial Ecology: Policy Framework and Implementation*; Prentice-Hall: Old Tappan, NJ, USA, 1999.
3. Dincer, I.; Rosen, M.A. *Exergy: Energy, Environment and Sustainable Development*; Elsevier: Oxford, UK, 2007.
4. Rosen, M.A.; Bulucea, C.A. Assessing Electrical Systems via Exergy: A Dualist View Incorporating Technical and Environmental Dimensions. In *Proceedings of the 6th WSEAS International Conference on Engineering Education (EE'09)*, Rhodes, Greece, 22–24 July 2009; pp. 116-123.
5. Nicola, D.A.; Rosen, M.A.; Bulucea, C.A.; Brandusa, C. Sustainable Energy Conversion in Electrically Driven Transportation Systems. In *Proceedings of the 6th WSEAS International Conference on Engineering Education (EE'09)*, Rhodes, Greece, 22–24 July 2009; pp. 124-132.
6. Koroneos, C.J.; Nanaki, E.A. Energy and Exergy Utilization Assessment of the Greek Transport Sector. *Resour. Conser. Recyc.* **2008**, *52*, 700-706.
7. Gasparatos, A.; El-Haram, M.; Horner, M. A Longitudinal Analysis of the UK Transport Sector, 1970–2010. *Energ. Policy* **2009**, *37*, 623-632.
8. Federici, M.; Ulgiati, S.; Basosi, R. A Thermodynamic, Environmental and Material Flow Analysis of the Italian Highway and Railway Transport Systems. *Energy* **2008**, *33*, 760-775.
9. Dispenza, C.; Dispenza, G.; La Rocca, V.; Panno, G. Exergy Recovery during LNG Regasification: Electric Energy Production—Part One. *Appl. Therm. Eng.* **2009**, *29*, 380-387.
10. Potter, S. Exploring Approaches towards a Sustainable Transport System. *Int. J. Sustain. Transp.* **2007**, *1*, 115-131.
11. Litman, T.; Burwell, D. Issues in Sustainable Transportation. *Int. J. Glob. Environ. Issues* **2006**, *6*, 331-347.
12. Hull, A. Policy Integration: What Will It Take to Achieve More Sustainable Transport Solutions in Cities. *Transport Policy* **2008**, *15*, 94-103.
13. Siu, L.K. Innovative Lightweight Transit Technologies for Sustainable Transportation. *J. Transp. Systems Eng. Inform. Technol.* **2007**, *7*, 63-70.

14. MacHaris, C.; Van Mierlo, J.; Van Den Bossche, P. Combining Intermodal Transport with Electric Vehicles: Towards More Sustainable Solutions. *Transp. Plan. Technol.* **2007**, *30*, 311-323.
15. Graedel, T.E.; Allenby, B.R. *Industrial Ecology*; Pearson Education: Upper Saddle River, NJ, USA, 2003.
16. Givoni, M.; Brand, C.; Watkiss, P. Are Railways “Climate Friendly”? *Built Environ.* **2009**, *35*, 70-86.
17. Nicola, D.A.; Cismaru, D.C. *Tractiune Electrica: Fenomene, Modele, Solutii (Electric Traction: Phenomena, Models, Solutions)*; SITECH Publishing House: Craiova, Romania, 2006.
18. Kaller, R.; Allenbach, J.M. *Traction Electrique (Electrical Traction)*; PPUR: Lausanne, Switzerland, 1995; Volumes 1, 2.
19. Ayres, R.U. Industrial Metabolism. In *Technology and Environment*; Ausubel, J.H., Sladovich, H.E., Eds.; National Academy Press: Washington, DC, USA, 1989; pp. 23-49.
20. Holling, C.S.; Schindler, D.W.; Walker, B.W.; Roughgarden, J. Biodiversity in the Functioning of Ecosystems. In *Biodiversity Loss*; Perrings, C., Maler, K.G., Folke, C., Holling, C.S., Jansson, B.O., Eds.; Cambridge University Press: Cambridge, UK, 1995; pp. 44-83.
21. Bulucea, C.A.; Nicola, D.A.; Brandusa, A.; Brandusa, C. Drive Systems in Underground Metro Saving Energy. In *Proceedings of the 3rd IASME/WSEAS International Conference on Energy & Environment*, Cambridge, UK, 23–25 February 2008; pp. 433-439.
22. Nicola, D.A.; Bulucea, C.A.; Cismaru, D.C.; Brandusa, C. Energy Saving in Electric Trains with Traction Induction Motors. In *Proceedings of the 4th IASME/WSEAS International Conference on Energy & Environment*, Cambridge, UK, 24–26 February 2009; pp. 226-232.
23. Brandusa, C. *Driving Systems with Static Converters and Induction Motors in Electric Urban Traction*; Ph.D. Thesis (in Romanian); University of Petrosani: Petrosani, Romania, 2007.